JOURNAL OF GEOPHYSICAL RESEARCH, VOL. 114, E00B28, doi:10.1029/2008JE003095, 2009

Modeling the distribution of H_2O and HDO in the upper atmosphere of Venus

Mao-Chang Liang[1,2] and Yuk L. Yung[3]

Received 31 January 2008; revised 30 June 2008; accepted 2 December 2008; published 24 February 2009.

[1] The chemical and dynamical processes in the upper atmosphere of Venus are poorly known. Recently obtained vertical profiles of trace species from the Venus Express mission, such as HCl, H_2O, and HDO, provide new information to constrain these processes. Here, we simulate these profiles, using the model we have developed and described in a related paper by Yung et al. (2008), with special emphasis on the modeling of H_2O and HDO. A new mechanism, the photo-induced isotopic fractionation effect (PHIFE) of H_2O and HCl, is incorporated into our model. The observed enhancement of HDO could be attributed to (1) preferential destruction of H_2O relative to HDO via PHIFE and (2) escape of hydrogen that enhances the abundance of D and hence its parent molecule HDO. Over a wide range of the sensitivity of the results to the changes of the two mechanisms, we find that the observed profiles of HDO and H_2O profiles cannot be explained satisfactorily by current knowledge of chemical and dynamical processes in this region of the atmosphere. Several conjectures to tackle the problems are discussed.

Citation: Liang, M.-C., and Y. L. Yung (2009), Modeling the distribution of H_2O and HDO in the upper atmosphere of Venus, *J. Geophys. Res.*, *114*, E00B28, doi:10.1029/2008JE003095.

1. Introduction

[2] Venus provides a window of opportunity in the solar system for studying the end-member of water evolution. Its highly enhanced D/H ratio, compared with the terrestrial value, suggests that about one Earth ocean might have been lost [e.g., *Kasting and Pollack*, 1983; *Donahue*, 1999, and references therein] via nonthermal escape of hydrogen (such as hydrodynamic escape, charge exchange, and collisionally induced escape). Hydrogen is produced by the photolysis of water, a process that is known to preferentially destroy the light isotopologue, resulting in the enrichment of the heavy parent molecule in the atmosphere [*Cheng et al.*, 1999]. The process of enhancing the abundance of parent molecules is similar in nonthermal escape of hydrogen, and hence over the course of Venusian history, the D/H ratio is enriched as compared with the primordial value. A combination of photolytic and nonthermal escape processes fractionates the ratio in a way faster than each of them alone. In this paper, we investigate the D/H ratio affected by the photo-induced isotopic fractionation effect (PHIFE) of H_2O/HDO and HCl/DCl in the present atmosphere of Venus. The reader is referred to *Miller and Yung* [2000] for a detailed explanation of PHIFE. The observed D/H in water in the upper atmosphere from Venus Express, along with other molecules (HCl, HF), provides additional constraints for understanding the relative importance of two dynamical processes: atmospheric circulation and escape. The former conserves the bulk D/H ratio in an air parcel and the latter enhances the ratio. As a result, the D/H ratio in water has less latitude dependence, compared with the case involving hydrogen escape. To evaluate the processes quantitatively in the upper atmosphere of Venus, one-dimensional (1-D) and two-dimensional (2-D) models are used. The data used for the study are described by *Bertaux et al.* [2007], *Vandaele et al.* [2008], and *Fedorova et al.* [2008].

2. Models

[3] One-dimensional photochemical models are used to simulate the vertical profiles of H_2O/HDO, HCl/DCl, H/D, H_2/HD, OH/OD, HO_2/DO_2, CO_2, CO, O_2, O, $O(^1D)$, O_3, Cl, ClO, Cl_2, ClCO, and $ClCO_3$ in the upper atmosphere (58–112 km) of Venus. The current model is based on *Yung and DeMore* [1982] and *Mills* [1998a, 1998b], and a subset of the chemistry is selected from *Yung et al.* [2008] to account for the UV attenuation in the upper part of the atmosphere. The selected hydrogen/deuterium chemistry is summarized in Table 1. The PHIFE of H_2O/HDO and HCl/DCl are taken from *Cheng et al.* [1999] and *Bahou et al.* [2001], respectively. The rest of the hydrogen and deuterium chemical reactions are assumed to be isotopically neutral. The transport and boundary conditions are primarily taken from *Yung and DeMore* [1982] and *Mills* [1998a, 1998b]. The CO_2 mixing ratio is relatively uniform at 0.96 throughout the entire atmosphere. The fixed mixing ratios of 1, 0.1, 0.15, and 0.0075 ppmv are used for H_2O, HDO, HCl, and DCl, respectively, at the lower boundary. The selected

[1]Research Center for Environmental Changes, Academia Sinica, Taipei, Taiwan.
[2]Graduate Institute of Astronomy, National Central University, Jhongli, Taiwan.
[3]Division of Geological and Planetary Sciences, California Institute of Technology, Pasadena, California, USA.

0148-0227/09/2008JE003095$09.00

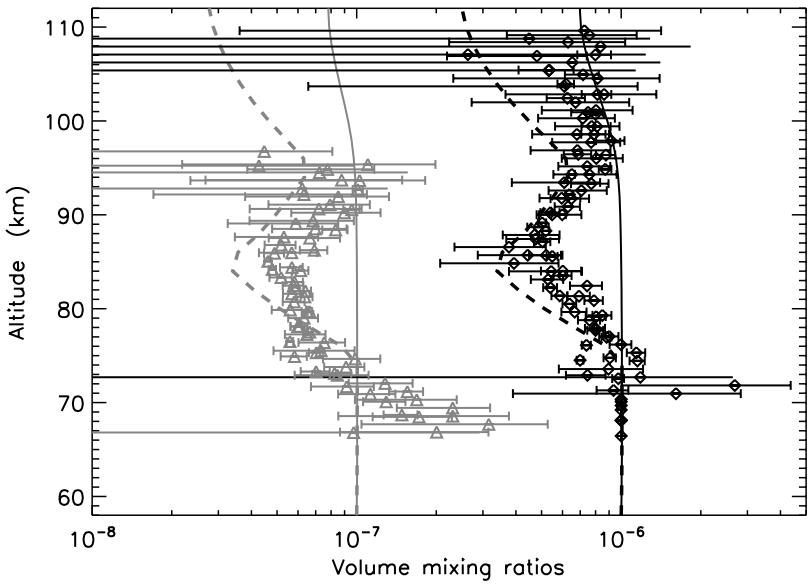

Figure 1. Modeled vertical profiles of H_2O (black) and HDO (gray) in 1-D model with prescribed winds depicted by solid and dashed curves (see text). Data are from *Bertaux et al.* [2007].

D/H ratio used to better represent the Venus Express profiles (Figure 1) is a factor of 2 higher than the bulk ratio, which is 0.05 for [HDO]/[H_2O]. The rest of the species are transported downward at the lower boundary at a velocity determined by dynamics; the velocities are 0.05 and 0.016 cm s^{-1} for 1-D and 2-D models, respectively. The upper boundary is impermeable to all species. This is chosen to be our reference case. A model with hydrogen escape is also run. In this model, species other than atomic H and D have zero flux at the upper boundary. The escape fluxes of H and D are, respectively, 3.5×10^6 and 3.1×10^4 atoms cm^{-2} s^{-1} [*Gurwell and Yung*, 1993] or higher [*Donahue*, 1999]. Sensitivity of the model results with respect to the changes of transport and upper boundary conditions is studied using the 1-D model. The UV radiation is averaged diurnally before photolytic calculations, and the latitude dependence is carefully taken into account. (See *Liang et al.* [2005, and references therein] for a detailed description of the model.) The modeled latitude for 1-D models is set at 45°N, where we think it should better represent the condition at the polar region if the time constant of the large-scale meridional circulation is not small compared with the time of vertical transport and the lifetimes of H_2O and HDO against photolysis. The major effect on the selection of the modeled latitude is the total photolysis rates (or J values) for molecules. The effect on isotopic ratios can be ignored under the current uncertainties of models and observations. We test the isotopic effect at a higher latitude at 80°N, and the largest difference of 5%, compared with that at 45°N, occurs above ~110 km.

[4] The 2-D version [*Liang et al.*, 2005] of the Caltech/JPL photochemical mode is employed to simulate the meridonal distribution of H_2O/HDO and HCl/DCl in the upper atmosphere of Venus. The current model and the adopted transport are described in a companion paper [*Yung et al.*, 2008]. We solve the model at latitudes from pole to pole and altitudes from 56 to 112 km. The chemical species and reactions are taken from the 1-D model described in the previous paragraph. The boundary conditions are the same as the 1-D case with hydrogen escape. This is selected to be our reference 2-D model.

[5] The vertical profile of H_2O provides insight into transport of the upper atmosphere of Venus. The SOIR data, taken near the north pole, show that H_2O mixing ratio decreases with increasing altitude until ~85 km and then increases above that [*Bertaux et al.*, 2007]. Since there is no known source and sink of this magnitude (~50%) above the cloud tops at ~50 km and below ~100 km (where photochemical processes become important), the profile has to be caused by transport. Several ad hoc advections have been tested, and 1-D models are used for such sensitivity study. One proposal that fits the data is having a downward advection (−0.3 cm s^{-1}) between 75 and 85 km and upwelling (0.5 cm s^{-1}) above until 95 km where the transport becomes downwelling (−0.5 cm s^{-1}). This qualitatively agrees with the fact that there is a temperature inversion layer at ~100 km. General circulation models [e.g., *Lee et al.*, 2007] predict, in general, that air ascends at low latitudes and descends at high latitudes (Hadley cell). The heating at ~100 km results from the wind profile (see later discussion on the relation between wind and temperature). The resulting H_2O and HDO profiles from this prescribed advection (dashed curves) are shown in Figure 1.

3. Results

[6] The photolysis of H_2O/HDO and HCl/DCl tends to enhance their isotopic composition δ, which is defined by the deviation of the ratio of an isotopically substituted species and its normal molecule from that of the prescribed standard

$$\delta \equiv [D]/[H]/([D]/[H])_0 - 1, \quad (1)$$

where [D] and [H] are the concentrations of [HDO] or [DCl] and [H_2O] or [HCl], respectively. The subscript "0" refers

Table 1. List of Hydrogen and Deuterium Chemical Reactions[a]

	Reaction	Rate Coefficient	Reference[b]
(R22)	$H_2O \rightarrow H + OH$	$J_{22} = 2.5 \times 10^{-6}$	4
(R25)	$HCl \rightarrow H + Cl$	$J_{25} = 1.8 \times 10^{-6}$	1
(R41)	$O(^1D) + H_2O \rightarrow 2OH$	$k_{41} = 2.2 \times 10^{-10}$	2
(R42)	$O(^1D) + H_2 \rightarrow H + OH$	$k_{42} = 1.1 \times 10^{-10}$	2
(R46)	$H + O_2 + CO_2 \rightarrow HO_2 + CO_2$	$k_{46} = 2.0 \times 10^{-31}\ (T/300)^{-1.6}$; $k_8 = 7.50 \times 10^{-11}$	2, 10
(R47)	$H + O_3 \rightarrow OH + O_2$	$k_{47} = 1.4 \times 10^{-10}\ e^{-470/T}$	2
(R49)	$O + HO_2 \rightarrow OH + O_2$	$k_{49} = 2.9 \times 10^{-11}\ e^{200/T}$	2
(R50)	$O + OH \rightarrow O_2 + H$	$k_{50} = 2.2 \times 10^{-11}\ e^{120/T}$	2
(R51)	$OH + CO \rightarrow CO_2 + H$	$k_{51} = 1.5 \times 10^{-13}$	8
(R52)	$OH + H_2 \rightarrow H_2O + H$	$k_{52} = 5.5 \times 10^{-12}\ e^{-2000/T}$	2
(R53)	$OH + O_3 \rightarrow HO_2 + O_2$	$k_{53} = 1.6 \times 10^{-12}\ e^{-940/T}$	2
(R54)	$HO_2 + O_3 \rightarrow OH + 2O_2$	$k_{54} = 1.1 \times 10^{-14}\ e^{-500/T}$	2
(R55)	$H + HO_2$? 2OH	$k_{55} = 7.3 \times 10^{-11}$	2
(R56)	$H + HO_2 \rightarrow H_2O + O$	$k_{56} = 1.6 \times 10^{-12}$	2
(R58)	$H + HO_2 \rightarrow H_2 + O_2$	$k_{58} = 6.4 \times 10^{-12}$	2
(R61)	$OH + HO_2 \rightarrow H_2O + O_2$	$k_{61} = 4.7 \times 10^{-11}\ e^{250/T}$	8
(R63)	$2H + CO_2 \rightarrow H_2 + CO_2$	$k_{63} = 5.0 \times 10^{-29}\ T^{-1.3}$	6, 9, 10
(R64)	$H + HCl \rightarrow H_2 + Cl$	$k_{64} = 1.5 \times 10^{-11}\ e^{-1750/T}$	10
(R65)	$OH + HCl \rightarrow Cl + H_2O$	$k_{65} = 2.6 \times 10^{-12}\ e^{-350/T}$	2
(R66)	$O + HCl \rightarrow OH + Cl$	$k_{66} = 1.0 \times 10^{-11}\ e^{-3300/T}$	2
(R67)	$Cl + H_2 \rightarrow HCl + H$	$k_{67} = 3.7 \times 10^{-11}\ e^{-2300/T}$	2
(R68)	$Cl + OH \rightarrow HCl + O$	$k_{68} = 1.2\ e^{-510/T}$	3
(R70)	$Cl + HO_2 \rightarrow HCl + O_2$	$k_{70} = 1.8 \times 10^{-11}\ e^{170/T}$	5
(R75)	$ClO + OH \rightarrow HO_2 + Cl$	$k_{75} = 1.1 \times 10^{-11}\ e^{120/T}$	8
(R78)	$Cl + H + M \rightarrow HCl + M$	$k_{78} = 1.0 \times 10^{-32}$	10
(R86)	$ClCO + H \rightarrow HCl + CO$	$k_{86} = 1.0 \times 10^{-11}$	10
(R90)	$H + Cl_2 \rightarrow HCl + Cl$	$k_{90} = 1.4 \times 10^{-10}\ e^{-90/T}$	3
(R91)	$Cl + HO_2 \rightarrow OH + ClO$	$k_{91} = 4.1 \times 10^{-11}\ e^{-450/T}$	5
(R95)	$ClCO_3 + H \rightarrow CO_2 + Cl + OH$	$k_{95} = 1.0 \times 10^{-11}$	10
(R104)	$O + H_2 \rightarrow OH + H$	$k_{104} = 9.9 \times 10^{-32}\ T^{6.5}\ e^{-1460/T}$	7
(R105)	$2OH \rightarrow H_2O + O$	$k_{105} = 4.2 \times 10^{-12}\ e^{-240/T}$	2
(R106)	$O(^1D) + HCl \rightarrow Cl + OH$	$k_{106} = 1.0 \times 10^{-10}$	8
(R115)	$O(^1D) + HCl \rightarrow O + HCl$	$k_{115} = 1.4 \times 10^{-11}$	8
(R116)	$O(^1D) + HCl \rightarrow H + ClO$	$k_{116} = 3.6 \times 10^{-11}$	8
(R127)	$ClO + H_2 \rightarrow HCl + OH$	$k_{127} = 1.0 \times 10^{-12}\ e^{-4800/T}$	8
(R128)	$O + H + M \rightarrow OH + M$	$k_{128} = 1.3 \times 10^{-29}\ T^{-1}$	8
(R130)	$H + OH + CO_2 \rightarrow H_2O + CO_2$	$k_{130} = 7.7 \times 10^{-26}\ T^{-2}$	8
(R139)	$HDO \rightarrow H + OD$	$\approx (1/2)J_{22}$	4
(R140)	$HDO \rightarrow D + OH$	$\approx (1/2)J_{22}$	4
(R141)	$DCl \rightarrow D + Cl$	$\approx J_{25}$	1
(R142)	$O(^1D) + HDO \rightarrow OH + OD$	k_{41}	assumed
(R143)	$O(^1D) + HD \rightarrow H + OD$	k_{42}	assumed
(R144)	$O(^1D) + HD \rightarrow D + OH$	k_{42}	assumed
(R146)	$D + O_2 + CO_2 \rightarrow DO_2 + CO_2$	k_{46}	assumed
(R147)	$D + O_3 \rightarrow OD + O_2$	k_{47}	assumed
(R149)	$O + DO_2 \rightarrow OD + O_2$	k_{49}	assumed
(R150)	$O + OD \rightarrow O_2 + D$	k_{50}	assumed
(R151)	$OD + CO \rightarrow CO_2 + D$	k_{51}	assumed
(R152)	$OD + H_2 \rightarrow HDO + H$	k_{52}	assumed
(R153)	$OH + HD \rightarrow HDO + H$	$(1/2)k_{52}$	assumed
(R154)	$OH + HD \rightarrow H_2O + D$	$(1/2)k_{52}$	assumed
(R155)	$OD + O_3 \rightarrow DO_2 + O_2$	k_{53}	assumed
(R156)	$DO_2 + O_3 \rightarrow OD + 2O_2$	k_{54}	assumed
(R157)	$D + HO_2 \rightarrow OH + OD$	k_{55}	assumed
(R158)	$H + DO_2 \rightarrow OH + OD$	k_{55}	assumed
(R159)	$D + HO_2 \rightarrow HDO + O$	k_{56}	assumed
(R160)	$H + DO_2 \rightarrow HDO + O$	k_{56}	assumed
(R163)	$D + HO_2 \rightarrow HD + O_2$	k_{58}	assumed
(R164)	$H + DO_2 \rightarrow HD + O_2$	k_{58}	assumed
(R168)	$OD + HO_2 \rightarrow HDO + O_2$	k_{61}	assumed
(R169)	$OH + DO_2 \rightarrow HDO + O_2$	k_{61}	assumed
(R171)	$D + H + CO_2 \rightarrow HD + CO_2$	k_{63}	assumed
(R172)	$D + HCl \rightarrow HD + Cl$	k_{64}	assumed
(R173)	$H + DCl \rightarrow HD + Cl$	k_{64}	assumed
(R174)	$OD + HCl \rightarrow Cl + HDO$	k_{65}	assumed
(R175)	$OH + DCl \rightarrow Cl + HDO$	k_{65}	assumed
(R176)	$O + DCl \rightarrow OD + Cl$	k_{66}	assumed
(R177)	$Cl + HD \rightarrow DCl + H$	$(1/2)k_{67}$	assumed
(R178)	$Cl + HD \rightarrow HCl + D$	$(1/2)k_{67}$	assumed
(R179)	$Cl + OD \rightarrow DCl + O$	k_{68}	assumed
(R181)	$Cl + DO_2 \rightarrow DCl + O_2$	k_{70}	assumed
(R182)	$ClO + OD \rightarrow DO_2 + Cl$	k_{75}	assumed
(R184)	$Cl + D + M \rightarrow DCl + M$	k_{78}	assumed

Table 1. (continued)

	Reaction	Rate Coefficient	Reference[b]
(R185)	$ClCO + D \rightarrow DCl + CO$	k_{86}	assumed
(R186)	$D + Cl_2 \rightarrow DCl + Cl$	k_{90}	assumed
(R187)	$Cl + DO_2 \rightarrow OD + ClO$	k_{91}	assumed
(R188)	$ClCO_3 + D \rightarrow CO_2 + Cl + OD$	k_{95}	assumed
(R189)	$O + HD \rightarrow OD + H$	$(1/2)k_{104}$	assumed
(R190)	$O + HD \rightarrow OH + D$	$(1/2)k_{104}$	assumed
(R191)	$OD + OH \rightarrow HDO + O$	k_{105}	assumed
(R192)	$O(^1D) + DCl \rightarrow Cl + OD$	k_{106}	assumed
(R193)	$OD + HCl \rightarrow HDO + Cl$	k_{110}	assumed
(R194)	$OH + DCl \rightarrow HDO + Cl$	k_{110}	assumed
(R195)	$DO_2 + HCl \rightarrow HDO + ClO$	k_{111}	assumed
(R196)	$HO_2 + DCl \rightarrow HDO + ClO$	k_{111}	assumed
(R197)	$O(^1D) + DCl \rightarrow O + DCl$	k_{115}	assumed
(R198)	$O(^1D) + DCl \rightarrow D + ClO$	k_{116}	assumed
(R200)	$ClO + HD \rightarrow DCl + OH$	$(1/2)k_{127}$	assumed
(R201)	$ClO + HD \rightarrow HCl + OD$	$(1/2)k_{127}$	assumed
(R202)	$O + D + M \rightarrow OD + M$	k_{128}	assumed
(R205)	$D + OH + CO_2 \rightarrow HDO + CO_2$	k_{130}	assumed
(R206)	$H + OD + CO_2 \rightarrow HDO + CO_2$	k_{130}	assumed

[a]The photolytic coefficients (J) are given for a diurnally averaged model at 45°N at the top of the atmosphere (s^{-1}). J value is defined by the product of the species' cross section and the solar spectrum. Two-body and three-body rate coefficients are given in units of $cm^3\ s^{-1}$ and $cm^6\ s^{-1}$, respectively.

[b]1, *Bahou et al.* [2001]; 2, *Baulch et al.* [1980]; 3, *Baulch et al.* [1981]; 4, *Cheng et al.* [1999]; 5, *Lee and Howard* [1982]; 6, *Prather et al.* [1978]; 7, *Robie et al.* [1990]; 8, *Sander et al.* [2006]; 9, *Trainor et al.* [1973]; 10, *Yung and DeMore* [1982].

to the reference standard, which is set at the lower boundary. Figure 2 shows the ratios of the photolytic coefficients (J values) of HDO/H_2O (black curve) and DCl/HCl (gray curve). The ratios decrease with decreasing altitude, demonstrating that their δ values can be enhanced accordingly by photolytic processes. The photolytic isotope fractionation studied in this article is caused primarily by self-shielding by the most abundant molecules. The photodissociation of H_2O occurs primarily at altitudes between ~80 and 110 km and that of HCl at altitudes less than ~70 km; the latter is more significant below ~95 km in terms of photolysis rate (Figure 3). In the regions below ~95 km, the photolysis of HCl provides a source of H atoms that eventually form H_2O. As this source favors the formation of H_2O over HDO, this results in a depletion of δ(HDO). The resulting column-averaged (above the lower boundary of 58 km) δ(HDO) is −2‰. As a result, HDO, HD, and D are all isotopically depleted; and δ(DCl) is enhanced by 25‰. The factor of ~10 between δ(HDO) and δ(DCl) is due to higher abundance of H_2O relative to HCl. Above 95 km, H_2O photolysis is significant and δ(HDO) increases with altitude. Including H_2O/HDO photolysis enhances its isotopic composition, and consequently, the total δ(HDO) above 58 km becomes −1‰ (Figure 4).

[7] Sensitivity of the results to atmospheric transport is shown by the dashed curves in Figures 1–4. Though the transport provides a good fit to the observed H_2O and HDO profiles, it is negligible in modifying δ(HDO). This is caused by a high eddy diffusion coefficient (a few times $10^5\ cm^2\ s^{-1}$, or a transport time of ~10^5 sec) that greatly dilutes the isotopic fractionation resulting from H_2O/HDO and HCl/DCl photolytic processes (see an explanation of the dilution effect by *Liang et al.* [2007]). Several other modifications in transport have been tested but none gives a satisfactory explanation to both H_2O and HDO profiles. For example, the decreasing mixing ratios of H_2O and HDO between 70 and 85 km can be caused by advection and diffusive separation. The former can be prescribed by a downwelling transport (adopted in this paper). The latter requires a reduction of eddy mixing coefficients (so that molecular diffusion becomes more important than advective transport). The increase above ~85 km can be attributed either to upwelling transport (adopted in this paper) or to downwelling of air from a higher region in the atmosphere where H_2O/HDO sources are needed. To account for the increase, the required H_2O source is $\gg 5 \times 10^8$ molecules $cm^{-2}\ s^{-1}$ (the total photolysis rate of H_2O approximately the photolysis rate of HCl above 85 km; Figure 4), a value that is unreasonably high. Furthermore, the increase of the ratio of $[HDO]/[H_2O]$ above ~70 km observed by Venus Express implies that either H_2O photolysis is not small (i.e., at least 0.1 times HCl photolysis) or a hitherto unknown mechanism that transports HDO to the region. Further a general circulation model with the correct physics (e.g., heating between 90 and 120 km) is urgently needed. The laboratory measurements of the photolytic cross sections of H_2O/HDO/HCl/DCl at temperatures (~150–200 K) similar to the Venus' are also required, because of the temperature-dependent nature of PHIFE [e.g., *Kaiser et al.*, 2002; *Liang et al.*, 2004].

[8] Additionally, atomic hydrogen can escape from the atmosphere of Venus. The escape fluxes of H and D are estimated to be 3.5×10^6 and 3.1×10^4 atoms $cm^{-2}\ s^{-1}$, respectively [*Gurwell and Yung*, 1993]. Higher fluxes determined by *Donahue* [1999] are also tested, but no noticeable effect is observed. This additional process, that enhances atomic D abundance (i.e., increase D/H ratio) in an air parcel, followed by subsequent chemical reactions of H/D with oxygen compounds favors the production of HDO. However, the escape flux is 2 orders of magnitude lower than the photolysis of H_2O/HDO and HCl/DCl. Consequently, the hydrogen escape plays a small role in modifying the isotopic composition of water. This effect is identical to the influx of water described in the previous paragraph.

[9] Figure 5 shows the modeled HDO/H_2O ratios in the 2-D model. The ratio is relatively uniform in the regions below ~95 km and increases above. The increase is caused by the preferential photolysis of H_2O over HDO, as de-

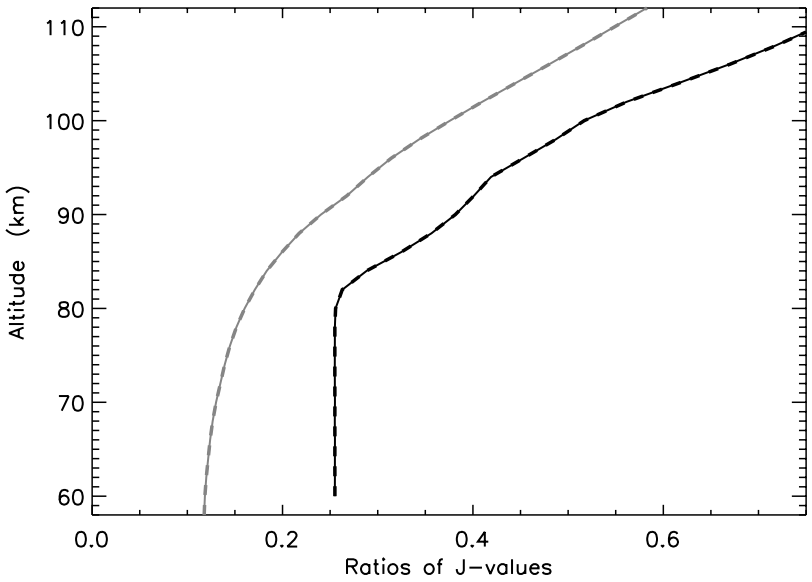

Figure 2. Ratios of the photolytic coefficients (J values) of deuterated and normal molecules. Black and gray curves are for the ratios of HDO/H_2O and DCl/HCl, respectively. Line designation is same as that in Figure 1. The solid and dashed curves are indistinguishable in the current plotting scale.

scribed above. In addition, we see that the ratio of HDO/H_2O also decreases with increasing latitude, demonstrating that in the current model, transport plays a negligible role in modifying the isotopic composition of water. As in the reference 1-D model, we obtain no kink feature in H_2O and HDO mixing ratio profiles observed by Venus Express. The transport was obtained by assuming Newtonian cooling [*Lee et al.*, 2007]. Future work on the transport is required.

4. Discussion

[10] In our standard 1-D model, the eddy diffusion coefficient in the upper atmosphere of Venus is $\sim 10^6$ cm^2 s^{-1}, and this corresponds to a mixing time $\sim 10^5$ s [see *Yung and DeMore*, 1982]. The prescribed advection transport has a time constant of $\sim 10^6$ s (velocity of 0.4 cm s^{-1} and atmospheric scale height of 4 km), an order of magnitude lower than the eddy mixing time. This confirms that the prescribed advection can explain well the vertical mixing ratio profile of H_2O but not the ratio profile of HDO/H_2O. We will demonstrate in section 4.2 that the tentatively observed enhancement of HDO relative to H_2O [*Bertaux et al.*, 2007] could be explained by the PHIFE of water alone, through hitherto unknown processes that transport the isotopic signature to a lower altitude. Moreover, our model also suggests that in order to explain the observed H_2O profile, an upward transport of 0.5 cm s^{-1} between 85 and 95 km and a downward transport of 0.5 cm s^{-1} above 95 km are needed. The existence of downward transport is supported by the temperature anomaly observed by Venus Express [*Bertaux et al.*, 2007] (see section 4.1), but the upward transport remains a puzzle. We note that though the temperature inversion is obtained on the night side at midlatitudes, this inversion probably extends to the polar region on the basis of the analogy with the terrestrial middle atmosphere [see, e.g., *Holton et al.*, 1995, Figure 3]. A 3-D general circulation model that includes realistic heating is urgently needed to resolve these issues.

4.1. Temperature Anomaly and Descent Rate

[11] SPICAV data show a large temperature anomaly $\sim$20–50 K at around 100 km, taken on the night side at low to midlatitudes [see *Bertaux et al.*, 2007, Figure 1]. The authors interpret this as evidence for heating by air subsidence. The associated vertical velocity may be estimated as follows. The thermodynamic equation can be written as follows [*Andrews et al.*, 1987, p. 115]:

$$DT/Dt + \kappa wT/H = J/C_p, \tag{2}$$

where D/Dt is material derivative, T is temperature, w is vertical velocity, H is scale height, J is diabatic heating rate, κ is $(\gamma - 1)/\gamma$, γ is C_p/C_v, and C_p and C_v are heat capacity at constant pressure and volume, respectively. For a CO_2 atmosphere, $\kappa = 1/4$. For vertical advection only, we have

$$DT/Dt = \partial T/\partial t + w\partial T/\partial z. \tag{3}$$

Substituting (3) into (2) and simplifying, we have

$$\partial T/\partial t + w(\partial T/\partial z + \kappa T/H) = J/C_p. \tag{4}$$

Since we are interested in dynamical heating, we can set $J = 0$. Equation (4) allows us to estimate the change of temperature due to dynamical heating

$$\Delta T = -w(\partial T/\partial z + \kappa T/H)\Delta t. \tag{5}$$

The maximum change in T occurs for $\Delta t = t_{\mathrm{rad}}$, where t_{rad} is the Newtonian cooling time constant [see, e.g., *Goody and Yung*, 1989, p. 252]. If $\Delta t \gg t_{\mathrm{rad}}$ cooling by radiation becomes important, thereby reducing the effect of dynami-

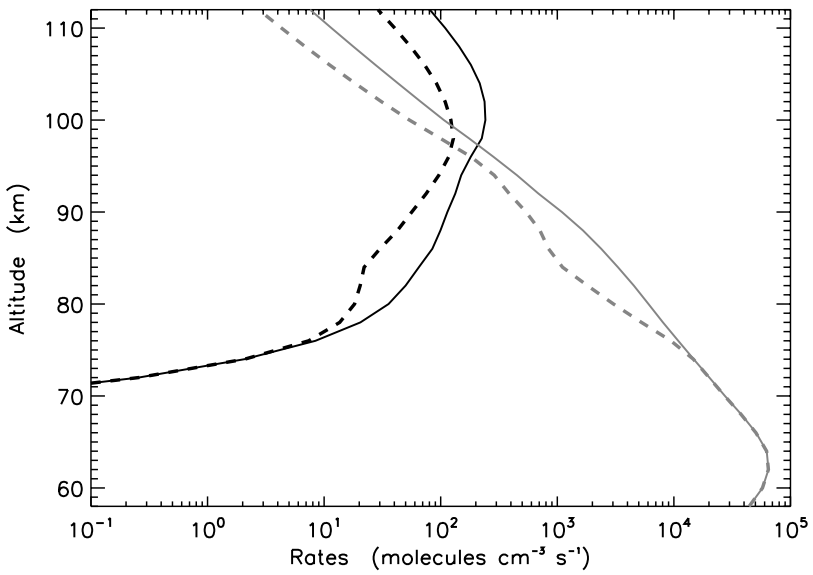

Figure 3. The photolysis rates of H_2O (black) and HCl (gray). Line designation is same as that in Figure 1.

cal heating. For Venus around 100 km (~0.03 hPa), we have the following values for the quantities in equation (5):

$$T = 175\text{K}, \tag{6}$$

$$\partial T/\partial z = -4\text{K/km}, \tag{7}$$

$$H = 4\text{km}, \tag{8}$$

$$\Delta t = t_{\text{rad}} \sim 1 \text{ day}, \tag{9}$$

where in (9), we have used estimates based on *Crisp and Titov* [1997]. Substituting (6)–(9) into (5) we have

$$\Delta T = -54w, \tag{10}$$

where the units for ΔT and w are K and cm s^{-1}, respectively. Thus, if we have downwelling velocity ~1 cm s^{-1}, then ΔT is ~54 K, which is also the correct order of magnitude to account for the H_2O profile, as discussed in the previous section. On the other hand, if we use the descent velocity of 0.43 m s^{-1} suggested by *Bertaux et al.* [2007], we have ΔT is ~2322 K, which is clearly too large compared with the observations! Thus, the H_2O profile offers a potentially valuable clue to the descent rate of air in the mesosphere of Venus.

4.2. Isotopic Enrichment

[12] SOIR data show evidence for changes in H_2O, HDO and the HDO/H_2O ratio. There appears to be a decrease in H_2O mixing ratio between 70 km and 85 km, even though the mixing ratio of H_2O or HDO could be seriously affected by the uncertainty in CO_2 retrieval, as pointed out by *Vandaele et al.* [2008]. This is explained as follows and summarized in Figure 6. The higher signal-to-noise ratio data are obtained at altitudes between ~75 and 85 km (blue symbols). An offset between the solid line and the blue symbols can be accounted for by the mixing ratio of H_2O and the ratio of [HDO]/[H_2O] set at the lower boundary. Both H_2O and HDO are destroyed by photolysis

$$\text{H}_2\text{O} + \text{hv} \rightarrow \text{OH} + \text{H}, \tag{11}$$

$$\text{HDO} + \text{hv} \rightarrow \text{OD} + \text{H}, \tag{12a}$$

$$\text{HDO} + \text{hv} \rightarrow \text{OH} + \text{D}. \tag{12b}$$

Let x and y be the concentrations of H_2O and HDO, respectively. In the absence of production, the loss of x and y is described by

$$dx/dt = -J_{11}x, \tag{13}$$

$$dy/dt = -J_{12}x, \tag{14}$$

where J_{11} and J_{12} denote the photodissociation coefficients for reactions (11) and (12). Solving these equations, we have

$$x(t) = x(0)\exp(-J_{11}t) \tag{15}$$

$$y(t) = y(0)\exp(-J_{12}t), \tag{16}$$

and

$$R(t) = [y(t)/x(t)]/[y(0)/x(0)] = \exp[(J_{11} - J_{12})t]. \tag{17}$$

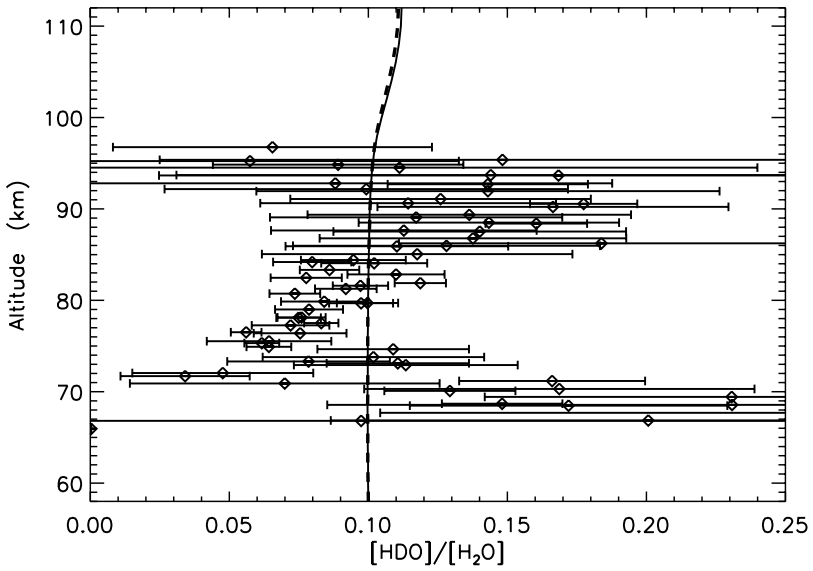

Figure 4. Model HDO/H_2O corresponding to cases in Figure 1. Data are from *Bertaux et al.* [2007]. The two curves are indistinguishable below ~100 km. Line designation is the same as that in Figure 1.

Let $r(t) = x(t)/x(0)$. From (15), we have

$$r(t) = \exp(-J_{11}t). \tag{18}$$

From (17) and (18), we can derive a simple relation

$$R(t) = [r(t)]^{-f}, \tag{19}$$

where

$$f = (J_{11} - J_{12})/J_{11}. \tag{20}$$

Referring to the data from SOIR, let us assume that the mixing ratio of H_2O at the cloud tops is 1 ppm; at 95 km, the value has decreased to 0.7 ppm. Therefore, $r(t) = 0.7$. From our model, $J_{12}/J_{11} = 0.54$; thus $f = 0.46$ (The total column integrated photolysis rates of HDO and H_2O are 2.6×10^7 and 4.8×10^8 molecules cm^{-2} s^{-1}, respectively, giving the averaged ratio of $J_{12}/J_{11} = 0.54$. Since the vertical transport time is significantly shorter than the photolytic lifetimes of H_2O and HDO, the column averaged J values are relevant to use.). The expected $R(t)$ from (19) is ~1.2, which is close to the observed enrichment between 70 and 75 km and 90–95 km. This simple theory offers a satisfactory explanation of the increase of the HDO/H_2O ratio as a result of the preferential destruction of H_2O relative to HDO. Figure 6 provides a quantitative prediction for the isotope ratio of water (R) to

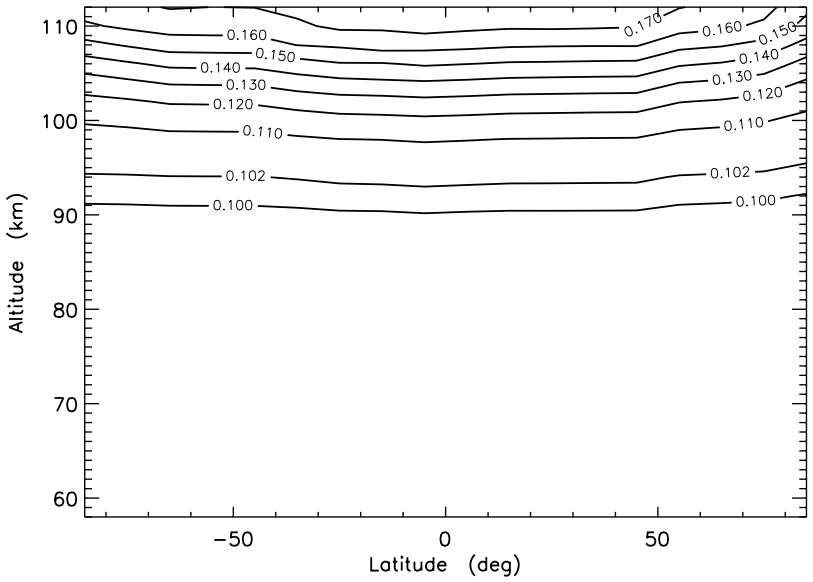

Figure 5. Reference case for simulation of the ratio of HDO and H_2O by the 2-D model.

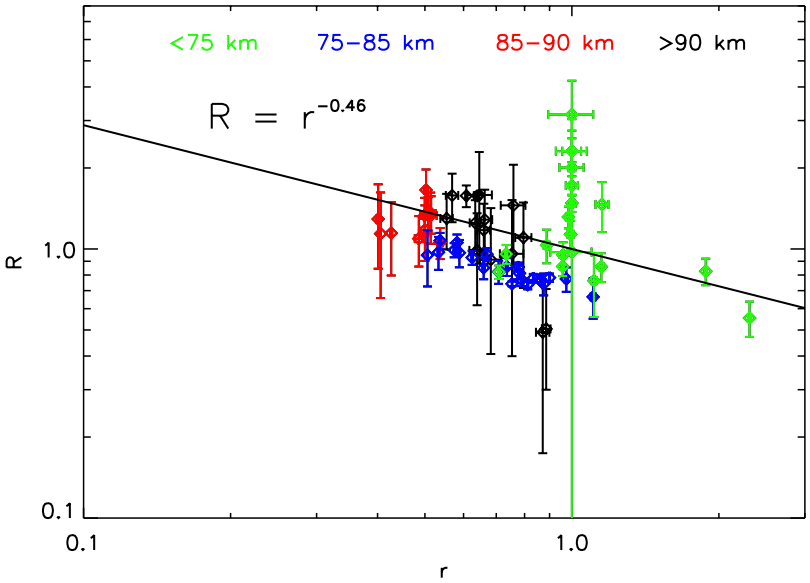

Figure 6. The isotope ratio of water (R) to the fraction of remaining water (r). See text for details.

the fraction of remaining water (r). This relation is consistent with the limited observations currently available. It is desirable to test this relation over a wider range of R and r.

5. Concluding Remarks

[13] Simple one-dimensional and two-dimensional chemistry and transport models are used to study the spatial distribution of HCl, H_2O, and HDO in the upper atmosphere of Venus. The distributions of these molecules in the atmosphere reflect the influence of chemistry and transport. A large subsidence at around 85 km is needed to explain the observed vertical profile of H_2O. The magnitude of the descent rate is consistent with the temperature anomaly observed by SPICAV. Preferential photolysis of H_2O over HDO provides a driving force for isotopic enrichment. Laboratory measurements of temperature-dependent cross sections for H_2O over HDO are needed. The correct simulation of the distribution of HCl, H_2O, and HDO ultimately requires a 3-D model. This paper identifies the most important physical and chemical processes that a model must incorporate.

[14] The emphasis of this work is in the region of the atmosphere above 70 km, where the H_2O abundance is $\sim$1 ppm. As the abundance of H_2O in the deep atmosphere is $\sim$100 ppm, there is another removal mechanism that is not related to photolysis. It is known that H_2SO_4 aerosols are formed above the cloud tops. They represent a net sink of SO_2 and H_2O, thereby explaining their rapid decrease with altitude above the cloud tops. We do not know whether this process can cause fractionation. Laboratory studies are needed to determine the fractionation associated with this chemical dehydration, if any occurs.

[15] **Acknowledgments.** Special thanks are due to J.-L. Bertaux for providing H_2O, HDO, HCl, and HF profiles from Venus Express. We thank H. Hartman, N. Heavens. K. F. Li, V. Natraj, C. Parkinson, R. L. Shia, and X. Zhang for critical comments. This research was supported in part by NSC grant 97-2628-M-001-001 to Academia Sinica and NASA grant NNX07AI63G to the California Institute of Technology.

References

Andrews, D. G., J. R. Holton, and C. B. Leovy (1987), *Middle Atmosphere Dynamics*, 489 pp., Academic Press, Orlando, Fla.

Bahou, M., et al. (2001), Absorption cross sections of HCl and DCl at 135–232 nanometers: Implications for photodissociation on Venus, *Astrophys. J.*, *559*(2), L179–L182, doi:10.1086/323753.

Baulch, D. L., et al. (1980), Evaluated kinetic and photochemical data for atmospheric chemistry, *J. Phys. Chem. Ref. Data*, *9*(2), 295–471.

Baulch, D. L., J. Duxbury, S. J. Grant, and D. C. Montague (1981), Evaluated kinetic data for high-temperature reactions, Vol. 4—Homogeneous gas-phase reactions of halogen-containing and cyanide-containing species, *J. Phys. Chem. Ref. Data*, *10*(Supplement 1), 1–721.

Bertaux, J. L., et al. (2007), A warm layer in Venus' cryosphere and high-altitude measurements of HF, HCl, H_2O and HDO, *Nature*, *450*, 646–649.

Cheng, B. M., et al. (1999), Photo-induced fractionation of water isotopomers in the Martian atmosphere, *Geophys. Res. Lett.*, *26*(24), 3657–3660, doi:10.1029/1999GL008367.

Crisp, D., and D. Titov (1997), The thermal balance of the Venus atmosphere, in *Venus II: Geology, Geophysics, Atmosphere, and Solar Wind Environment*, edited by S. W. Bougher, D. M. Hunten, and R. J. Phillips, pp. 353–384, Univ. of Ariz. Press, Tucson, Ariz.

Donahue, T. M. (1999), New analysis of hydrogen and deuterium escape from Venus, *Icarus*, *141*(2), 226–235, doi:10.1006/icar.1999.6186.

Fedorova, A., O. Korablev, A.-C. Vandaele, J.-L. Bertaux, D. Belyaev, A. Mahieux, E. Neefs, W. V. Wilquet, R. Drummond, F. Montmessin, and E. Villard (2008), HDO and H_2O vertical distributions and isotopic ratio in the Venus mesosphere by Solar Occultation at Infrared spectrometer on board Venus Express, *J. Geophys. Res.*, *113*, E00B22, doi:10.1029/2008JE003146.

Goody, R. M., and Y. L. Yung (1989), *Atmospheric Radiation: Theoretical Basis*, Oxford Univ. Press, New York.

Gurwell, M. A., and Y. L. Yung (1993), Fractionation of hydrogen and deuterium on Venus due to collisional ejection, *Planet. Space Sci.*, *41*(2), 91–104, doi:10.1016/0032-0633 (93)90037-3.

Holton, J. R., P. H. Haynes, M. E. McIntyre, A. R. Douglass, R. B. Rood, and L. Pfister (1995), Stratosphere-troposphere exchange, *Rev. Geophys*, *33*(4), 403–439.

Kaiser, J., T. Rockmann, and C. A. M. Brenninkmeijer (2002), Temperature dependence of isotope fractionation in N_2O photolysis, *Phys. Chem. Chem. Phys.*, *4*(18), 4420–4430, doi:10.1039/b204837j.

Kasting, J. F., and J. B. Pollack (1983), Loss of water from Venus. Part 1. Hydrodynamic escape of hydrogen, *Icarus*, *53*(3), 479–508, doi:10.1016/0019-1035 (83)90212-9.

Lee, Y. P., and C. J. Howard (1982), Temperature-dependence of the rate-constant and the branching ratio for the reaction Cl+HO_2, *J. Chem. Phys.*, *77*(2), 756–763, doi:10.1063/1.443892.

Lee, C., S. R. Lewis, and P. L. Read (2007), Superrotation in a Venus general circulation model, *J. Geophys. Res.*, *112*, E04S11, doi:10.1029/2006JE002874.

Liang, M. C., G. A. Blake, and Y. L. Yung (2004), A semianalytic model for photo-induced isotopic fractionation in simple molecules, *J. Geophys. Res.*, *109*, D10308, doi:10.1029/2004JD004539.

Liang, M. C., et al. (2005), Meridional transport in the stratosphere of Jupiter, *Astrophys. J.*, *635*(2), L177–L180, doi:10.1086/499624.

Liang, M. C., G. A. Blake, B. R. Lewis, and Y. L. Yung (2007), Oxygen isotopic composition of carbon dioxide in the middle atmosphere, *Proc. Natl. Acad. Sci. U.S.A.*, *104*(1), 21–25, doi:10.1073/pnas.0610009104.

Miller, C. E., and Y. L. Yung (2000), Photo-induced isotopic fractionation, *J. Geophys. Res.*, *105*(D23), 29,039–29,051.

Mills, F. P. (1998a), Observations and photochemical modeling of the Venus middle atmosphere, Ph.D. thesis, Calif. Inst. of Technol, Pasadena, Calif.

Mills, F. P. (1998b), Thermal infrared spectroscopy of Europa and Callisto, Ph.D. thesis, Calif. Inst. of Technol, Pasadena, Calif.

Prather, M. J., J. A. Logan, and M. B. McElroy (1978), Carbon-monoxide in Jupiter's upper-atmosphere: An extraplanetary source, *Astrophys. J.*, *223*(3), 1072–1081, doi:10.1086/156340.

Robie, D. C., S. Arepalli, N. Presser, T. Kitsopoulos, and R. J. Gordon (1990), The intramolecular kinetic isotope effect for the reaction $O(^3P)$+HD, *J. Chem. Phys.*, *92*(12), 7382–7393, doi:10.1063/1.458224.

Sander, S. P., et al. (2006), Chemical kinetics and photochemical data for use in atmospheric studies, *Jet Propul. Lab. Pub. 06–2*, Jet Propul. Lab., Pasadena, Calif. (Available at http://jpldataeval.jpl.nasa.gov/.)

Trainor, D. W., D. O. Ham, and F. Kaufman (1973), Gas-phase recombination of hydrogen and deuterium atoms, *J. Chem. Phys.*, *58*(10), 4599–4609, doi:10.1063/1.1679024.

Vandaele, A. C., et al. (2008), Composition of the Venus mesosphere by SOIR on board Venus Express, *J. Geophys. Res.*, *113*, E00B23, doi:10.1029/2008JE003140.

Yung, Y. L., and W. B. DeMore (1982), Photochemistry of the stratosphere of Venus: Implications for atmospheric evolution, *Icarus*, *51*(2), 199–247, doi:10.1016/0019-1035(82)90080-X.

Yung, Y. L., M. C. Liang, X. Jiang, C. Lee, B. Bezard, and E. Marcq (2008), Modeling the distribution of OCS in the lower atmosphere of Venus, *J. Geophys. Res.*, doi:10.1029/2008JE003094, in press.

M.-C. Liang, Research Center for Environmental Changes, Academia Sinica, 128 Academia Road, Section 2, Taipei 115, Taiwan. (mcl@rcec.sinica.edu.tw)

Y. L. Yung, Division of Geological and Planetary Sciences, California Institute of Technology, MC 170-25, 1200 East California Boulevard, Pasadena, CA 91125, USA.